

Cz-Si wafers in solar cell production: Efficiency-limiting defects and material quality control

Jonas Haunschild, Juliane Broisch, Isolde Reis & Stefan Rein, Fraunhofer Institute for Solar Energy Systems (ISE), Freiburg, Germany

ABSTRACT

Most high-efficiency solar cells are fabricated from monocrystalline Czochralski silicon (Cz-Si) wafers because the material quality is higher than multicrystalline silicon (mc-Si) wafers. However, the material study presented in this paper reveals strong variations in the material quality of commercially available Cz-Si wafers, leading to a loss in solar cell efficiency of 4% absolute. The reason for this is the presence of defects, which appear as dark rings in photoluminescence (PL) images of the finished solar cells. It is shown that these efficiency-limiting defects originate from oxygen precipitation during emitter diffusion. It is demonstrated that an incoming inspection in the as-cut state is difficult, as strong ring structures in as-cut wafers turn out to originate most often from thermal donors. These are dissolved during high-temperature treatments and are therefore harmless, whereas moderate ring structures in the as-cut state may become severe. That is why critical wafers can be identified and sorted out reliably only after emitter diffusion, by using QSSPC-based lifetime measurements or PL imaging. The two-year statistics gathered from the research line at Fraunhofer ISE on the occurrence of ring defects in Cz-Si wafers indicate that ring defects are highly relevant in terms of material yield.

Introduction

It was only six years ago that Fuyuki et al. [1] and Trupke et al. [2] proposed electro- and photoluminescence imaging (EL, PL) as characterization tools for solar cells and wafers. Since then, these techniques have become widely used. According to the yearly market survey by PHOTON [3], the number of companies selling EL tools is increasing and new companies are entering the market in the field of PL. Luminescence imaging owes its success to the fact that it is a very fast and non-destructive technique which allows electrical parameters to be characterized with high spatial resolution [4,5]. Defects do not appear as a single value, but as a pattern in the images. With knowledge of the specific pattern caused by a certain defect, the images can be interpreted in terms of physics, which allows a more precise quality and process control [6].

One of the most promising applications for PL imaging is the incoming quality control (IQC) of multicrystalline silicon (mc-Si) wafers in the as-cut state. In IQC all wafers whose mechanical or electrical quality is not sufficient for producing high-performance solar cells should be rejected or sorted into an adequate production process. However, in the as-cut state, bulk lifetime information is highly masked by surface recombination due to the saw damage of the wafers and is therefore almost invisible to state-of-the-art characterization tools. Approaches for overcoming this problem are currently being researched [7,8]. The limited lifetime information is also an issue for PL imaging,

but fortunately most electrical defects formed during crystallization appear as very distinct patterns in PL images. By applying pattern recognition, it has been shown that open-circuit voltage, short-circuit current and efficiency can be predicted for a known solar cell process [9,10]. Current research aims at establishing a reliable wafer rating based on an automatic evaluation of PL images which can be acquired with high resolution at in-line speed.

In general, material quality of Czochralski-grown monocrystalline silicon (Cz-Si) is higher than that of multicrystalline silicon (mc-Si). That is why PL-based IQC has so far focused on mc-Si. However, recent studies have revealed that material quality in Cz-Si wafers may differ significantly as well [11,12]. Particularly when using Cz-Si wafers for high-efficiency solar cell concepts exceeding 20% efficiency, minor defects can already limit cell performance [13]. It has to be emphasized that the defects observed in these studies and discussed in this paper do not relate to the well-known metastable defect formed by boron–oxygen pairing (BO) [14,15], but rather to more severe background defects.

In a recent study [12,16] the varying impact of such oxygen-related defects on solar cell performance was evaluated and the possibility of detecting them by means of in-line measurements was investigated. The present paper gives an overview of these results and adds some new results from ongoing work. First, a short overview is given on oxygen-

related defects, the material compilation underlying this study and the solar cell process applied. Before investigating the possibilities of detecting severe ring defects by different characterization techniques in different process steps, the impact of ring defects on the efficiency of finished solar cells will be demonstrated. Finally, new results concerning the identification of oxygen precipitates as the main defect are presented, together with data about the statistical relevance of these defects for the PV industry.

“The most prominent defects are thermal donors, which strongly influence resistivity measurements, and the metastable boron–oxygen complex, which leads to light-induced degradation in the final solar cells.”

Oxygen-related defects in Cz-Si

Oxygen-related defects in Cz-Si have been characterized thoroughly for semiconductor devices [17,18]. The impact of these types of defect on solar cell performance is currently gaining in importance, as highly efficient solar cell concepts require materials of the highest

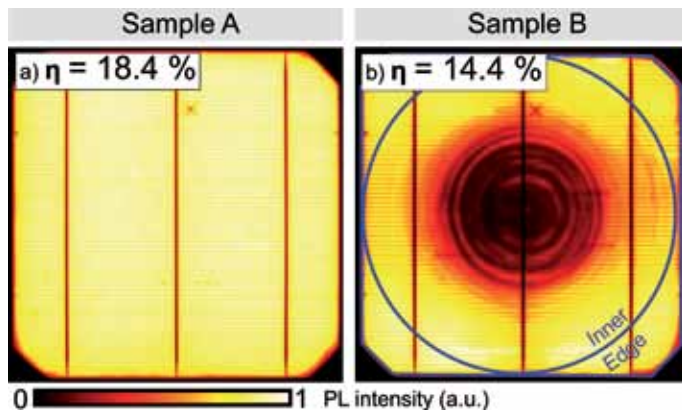


Figure 1. PL images of two finished solar cells: (a) sample A, which yielded 18.4% efficiency, with no rings present; (b) sample B, which yielded only 14.4% efficiency, showing pronounced rings.

quality. Typical oxygen concentrations in Cz-Si are of the order of 10^{17} – 10^{18} cm⁻³. Oxygen enters into the silicon melt primarily by out-diffusion from the quartz crucible and is built into the silicon lattice during crystallization. Depending on temperature gradients and pulling speed during crystallization, interstitial- and vacancy-rich regions can form. These intrinsic defects have direct and different impacts on oxygen precipitation and the formation of oxygen defects [19]. The variety of these oxygen-related defects is wide and their influence on carrier lifetime varies. They can be activated and deactivated by high-temperature steps, depending on the plateau temperatures and the heating and cooling ramps of the high-temperature steps applied during solar cell processing. The most prominent defects are thermal donors [20,21], which strongly influence resistivity measurements, and the metastable boron–oxygen complex [14,15], which leads to light-induced degradation in the final solar cells.

In semiconductor technology, oxygen precipitation is another well-known effect [22,23]. If uncontrolled, precipitation may lead to severe defects which can cause failure of integrated circuits. However, by applying special thermal treatments during production, precipitate growth can be carefully controlled to take place only in the bulk, and impurities are gettered from the regions near the surface, thus increasing material quality in the so-called ‘denuded zone’. In photovoltaics, however, both the bulk and the surface need to be free of precipitates. The formation of oxygen precipitates has only recently been observed with respect to solar cells [24], and has not yet been investigated in depth.

Pre-characterization and solar cell processing

Definition of suitable IQC measures for Cz-Si first requires a representative

picture of the defect classes present in Cz-Si. To obtain this, Cz-Si wafers were investigated from different crystal positions, manufacturers and crystallization processes within a broad material evaluation. Two hundred wafers with resistivities specified in the range 1–6 Ωcm were grouped in different quality classes according to their appearance in the PL image taken in the as-cut state. Half of the wafers were fabricated into solar cells using a standard 156mm × 156mm solar cell process, which included alkaline texturing, two-sided emitter diffusion, phosphorus silicate glass etching, antireflection coating, screen-printing, fast firing and laser-edge isolation. The other half of the wafers, consisting of wafers adjacent to the processed wafers, were used for a more detailed characterization. Solar cells whose efficiency was limited by process-induced defects such as shunts or high series resistances were identified by applying thermographical measurements

and quantitative PL imaging [25] and were excluded from the study in order to focus only on material-related issues.

PL imaging was performed on the setup build at Fraunhofer ISE, where a laser at 790nm irradiates the sample area with an illumination equivalent to up to two suns. The radiative band-to-band recombination of the excited charge carriers is detected by means of a Si-CCD camera with appropriate filters mounted in front of the camera lens to block reflected excitation light.

Efficiency-limiting defects in Cz-Si solar cells

The results from *I-V* curve measurements reveal that the efficiency ranges from 14.4% up to 18.4% in the non-degraded state. PL images of a solar cell with a high efficiency and with a low efficiency are shown in Fig. 1. As process-related problems can be excluded, efficiency is limited by the ring-like defect structure, which is highly recombination active and thus appears dark in the PL image of sample B in Fig. 1. The observed efficiency drop of 4% (absolute) can thus be attributed to poor material quality.

In order to find out if the differences in efficiency scale with the intensity of the rings visible in PL images, a simple metric – ring defect strength (RDS) – was set up in which the mean count rates of the edge region of the luminescence signal were divided by the mean count rates of the inner region under open-circuit conditions, as marked in Fig. 1(b). Both regions are symmetric with respect to the centre of the solar cells. The position of the circle was chosen to cover the largest extension of rings in this study and is applied to all solar cells. Note that this procedure is only feasible if the PL image is not completely covered by rings.

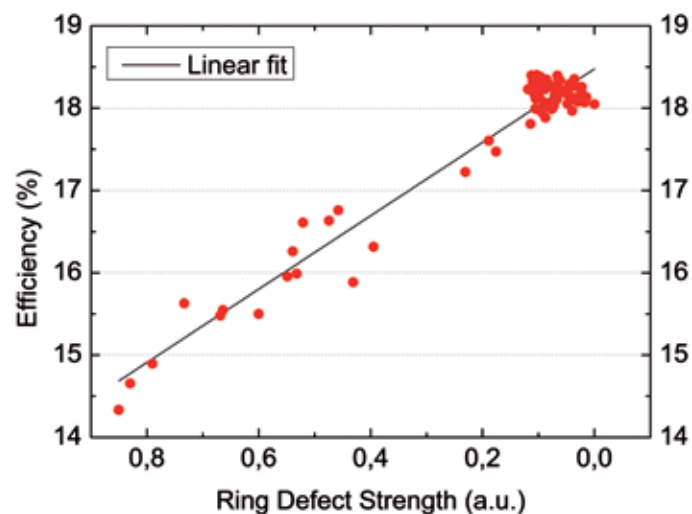


Figure 2. Solar cell efficiency as a function of the ring defect strength (defined as the ratio of the average PL-intensities in the centre and the edge region shown in Fig. 1b) measured for finished Cz-Si solar cells.

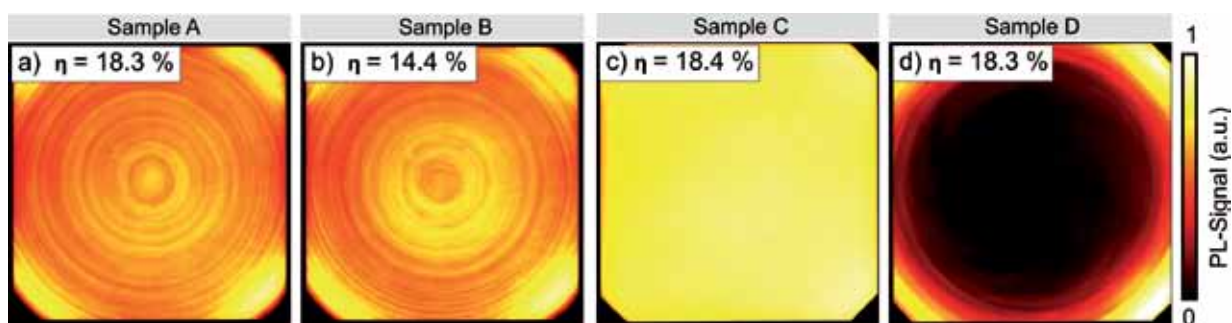


Figure 3. PL images of Cz-Si as-cut wafers: a typical homogeneous image is shown in (c), while different kinds of ring patterns are shown in (a), (b) and (d). The rings are caused by lateral differences in lifetimes and doping levels. The efficiencies represent the values of the finished solar cells processed from these wafers.

The ring defect strength is expressed as:

$$RDS = \frac{\langle I_{PL}(x,y) \rangle_{Edge}}{\langle I_{PL}(x,y) \rangle_{Inner}} \quad (1)$$

Fig. 2 shows the correlation of RDS to the solar cell efficiency, with a correlation coefficient of $R^2 = 0.94$. The loss of efficiency in this batch can be therefore clearly attributed to material defects within the Cz-Si wafers which appear as concentric ring-like defect patterns in the PL images.

“Strong material defects have been found in commercially available Cz wafers labelled as ‘high quality.’”

It should be stressed that strong material defects have been found in commercially available Cz wafers labelled as ‘high quality’. The difference in efficiencies of 4% absolute is not tolerable for industrial solar cell processing. High-efficiency solar cell concepts in particular can be expected to suffer even more if material quality limits the efficiency to below 15%. Now two questions arise:

1. Can these defects be detected in the early stages of production so that a reliable IQC can allow the wafers in question to be directly rejected?
2. What is their physical origin?

Defect characteristics in different productions states

As-cut characteristics

When characterizing Cz-Si wafers by PL, the resulting image is expected to look homogeneous, because no major material defects should be present. However, a random sampling from wafers

from the storage at Fraunhofer ISE has revealed different kinds of ring- and swirl-structures. Four representative samples are presented in Fig. 3, along with their solar cell efficiencies. The images in Figs. 3(a) and 3(b) are the same samples as in Fig. 1 (but in the as-cut state here). Although the resulting efficiencies were quite different, both of these PL images show rings of medium intensity. Sample C in Fig. 3(c) looks homogeneous, as do most PL images of Cz-Si as-cut wafers, and resulted in a high efficiency. Fig. 3(d) shows bright edges, with the centre yielding almost no signal, but the finished solar cell surprisingly had a high efficiency.

All wafers in the batch can be sorted into one of four groups corresponding to the PL images in Fig. 3. Group A shows medium rings, resulting in high solar cell efficiency. Group B, also having medium rings but resulting in low efficiency, will be the main focus. Wafers from group C show no rings and result in high efficiency, while group D wafers have strong rings, but also result

in highly efficient solar cells. It would be desirable to identify wafers with a material quality during incoming inspection that is too low (group B), in order to allow their direct rejection or their transfer to specially adjusted production lines. Fig. 3 demonstrates that this is not possible solely by PL imaging, as groups A and B yield the same ring pattern.

In Fig. 4(a), solar cell efficiency is plotted as a function of the effective charge carrier lifetime measured on the individual wafers in the as-cut state using the quasi-steady state photoconducance (QSSPC) technique. With the in-line setup used, the measurement is performed on a coil with a diameter of 55mm in the centre of the wafer, and the lifetime values are extracted at an injection density $\Delta n = 5 \times 10^{14} \text{ cm}^{-3}$. The four wafer groups A–D are marked on the graph. For groups A and C, with as-cut lifetimes in the range of $0.7 \mu\text{s}$, the small differences in carrier lifetime do not correlate to small differences in cell

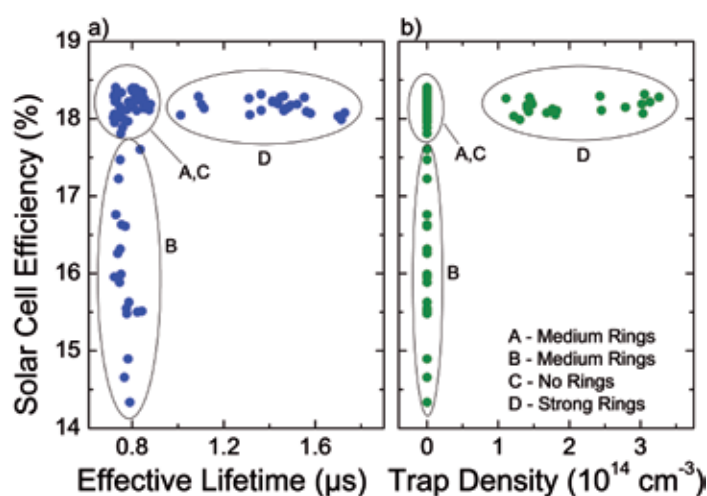


Figure 4. (a) Solar cell efficiency as a function of effective carrier lifetime, measured by means of QSSPC on the as-cut wafers; (b) cell efficiency as a function of trap density. Lifetime is limited by surface recombination and increased by charge carrier trapping, which may be corrected.

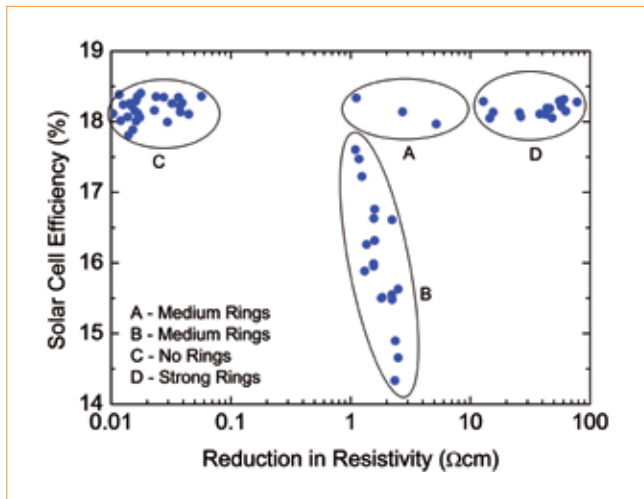


Figure 5. Reduction in resistivity after annealing plotted against solar cell efficiency. Wafers from group C show the noise of the measurement, while resistivities of groups A, B and D are reduced by more than 1Ωcm.

efficiency. In this case the lifetime of the finished cell is obviously high enough to reach the efficiency limit of the process. For group B, with as-cut lifetimes in the same range, cell efficiencies vary significantly, from 14.4% to 17.6%, which is not reflected in the lifetimes in the as-cut state. Group D wafers, with high as-cut lifetimes above 1.0μs, did not result in higher efficiencies.

In Fig. 4(b) trap density, extracted according to Sinton et al. [8], shows that the lifetime values of group D are increased by trapping artefacts, which cannot be completely removed despite a trapping correction, while wafers from groups A–C are not affected by trapping.

As in the case of PL imaging, lifetime measurements and the investigation of trap density do not allow a distinction to be made between groups A and B. This inability to distinguish between the groups is a result of either the surface limitation of carrier lifetime or a defect activation at a later process stage. If this is the case, the harmful effect from group B wafers may not be detected unambiguously in the as-cut state. Further research is required in this area.

Check for thermal donors

An in-line measurement of the base resistance yields values between 1.19 and 82.7Ωcm, which falls outside the material specification (1–6Ωcm). Increased and inhomogeneous resistance values of as-cut wafers are (in most cases) caused by the well-known thermal donor (TD) defect. TDs can be destroyed in a high-temperature step (e.g. emitter diffusion) and should have no effect on final solar cell results.

The results of an in-line test before and after a thermal treatment, performed in an in-line furnace with a peak temperature of 800°C for 10 seconds, are plotted in Fig. 5. After the treatment, all TDs had dissolved and resistivity for all tested wafers was in the expected range. The graph shows the absolute reduction in resistivity after annealing plotted against the solar cell efficiency. If no rings in the PL images are present (group C), the resistivity of the wafers does not change significantly, whereas the change for wafers from groups A and B is of the order of 1–10Ωcm; for group D the difference is greater than 10Ωcm. Therefore, we can conclude that Groups A and B have weak TDs, group C has no TDs and group D has strong TDs.

Although groups A and B cannot be distinguished by their changes in resistivity, the rings in the PL images of group A vanish, while they get stronger for group B. The same effect occurs after emitter diffusion and is discussed in the following section.

Characterization after emitter diffusion

Fig. 6 shows the PL images of the wafers from Fig. 3 in the as-cut state and the same wafers after emitter diffusion. Wafers from group A give homogeneous PL images, leading to the conclusion that the

PVA TePla AG is a leading crystal growing system provider for high-tech industries. The company has all industrially relevant methods (CZ, FZ, EFG and VGF) for crystal growing, particularly for growing mono- and multicrystalline silicon crystals.

Since 1958 over 1000 systems have been delivered and it is this longtime experience that PVA TePla and their customers benefit from. The company acts not only as a provider of high-quality systems made in Germany, but is also actively involved in the latest technological developments in crystal growing. Working together with our customers and research institutes, our in-house laboratory CCIC provides reliable support and outstanding solutions.

We know by heart that only our customers` success can be our own success!



CRYSTALLIZE YOUR VISIONS
WITH

PVA TePla

Im Westpark 10 - 12, 35435 Wettenberg, Germany
www.pvatepla.com, info@pvatepla.com,
Phone +49-641-68690-0, fax +49-641-68690-800

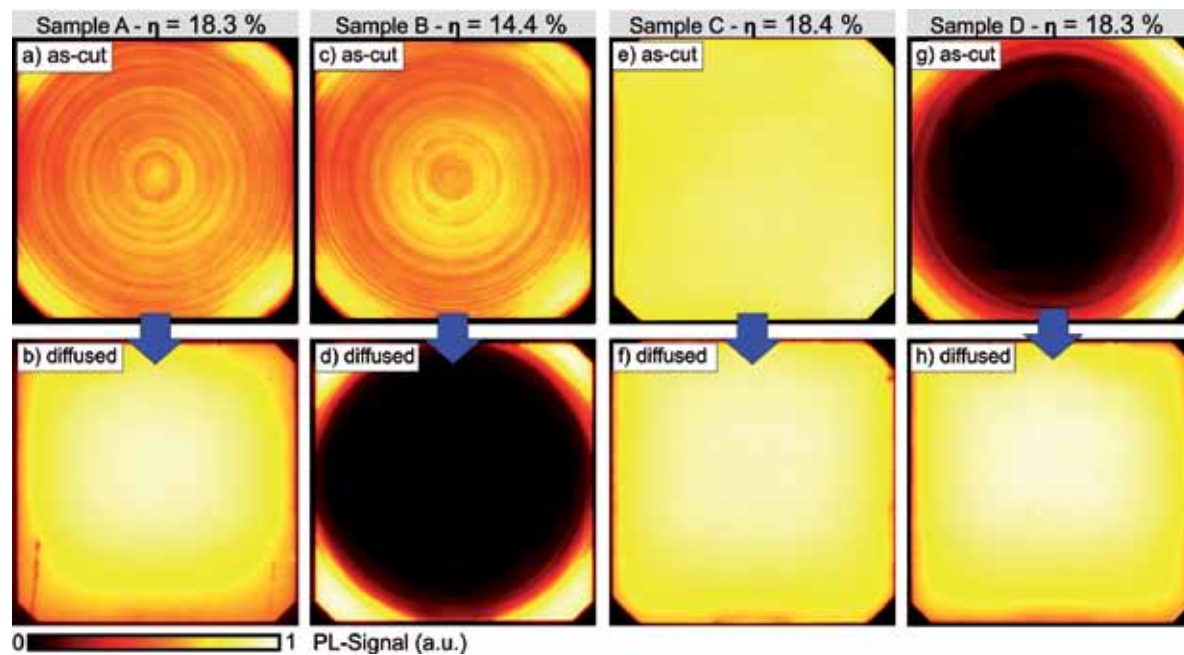


Figure 6. PL images of the as-cut wafers (the same ones as in Fig. 3) are displayed in the top row and PL images of the same wafers after emitter diffusion are displayed underneath. Whereas the rings vanish for samples A and D, they become stronger for sample B.

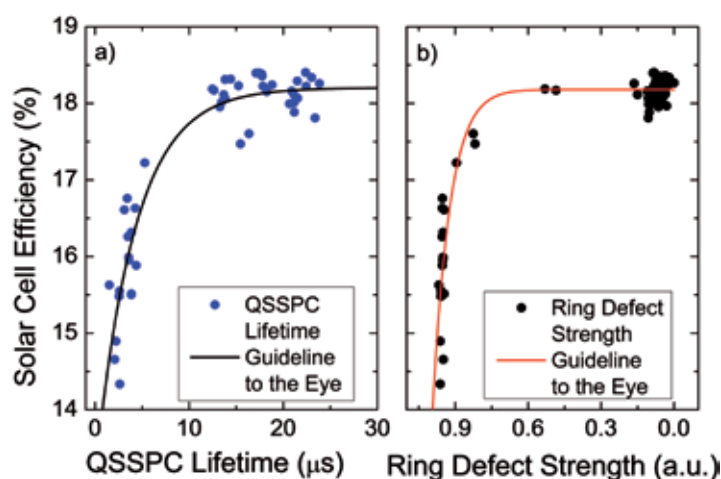


Figure 7. Solar cell efficiency plotted against (a) QSSPC lifetime, and (b) PL RDS, both measured after emitter diffusion. Wafers resulting in low efficiency can be identified reliably using both methods.

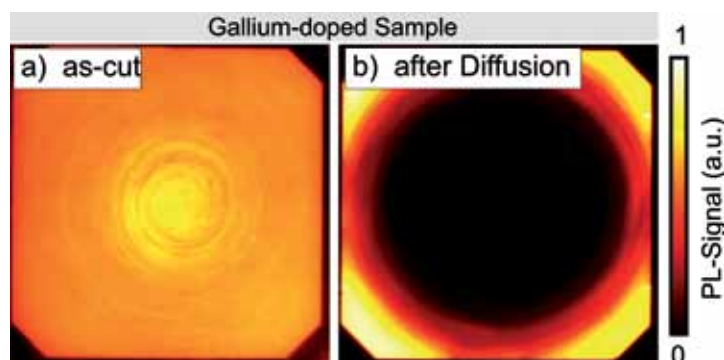


Figure 8. PL images of a Ga-doped Si wafer: (a) in the as-cut state; (b) after emitter diffusion.

ring effect in the as-cut state was caused by weak TDs. Wafers from group B, however, give a PL image with a dark centre of low lifetime. In addition to weak TDs, a more severe background defect must be present, which is activated during high-temperature processing. Group C wafers show no change, while the very dark rings of group D vanish. Pronounced rings in PL images of as-cut wafers can therefore be attributed to strong but harmless TDs.

Fig. 7 shows the solar cell efficiencies plotted as a function of the effective lifetime obtained from in-line QSSPC (Fig. 7a), and as a function of the ring defect strength extracted from PL images (Fig. 7b), both quantities measured after emitter diffusion. While low efficiencies can obviously be attributed to low carrier lifetimes, above approximately $20\mu\text{s}$ the cell efficiency is limited by the solar cell process. The PL RDS evaluation yields similar results and confirms that the low lifetimes originate from ring features. Therefore, both methods can be used for rating a wafer after emitter diffusion.

Dopant dependency

In addition to the investigation of the boron-doped samples, a group of gallium-doped silicon wafers was analysed. As shown in Fig. 8(a), ring patterns were found in the PL images of the as-cut wafers during incoming inspection. After emitter diffusion (Fig. 8b), a circular low-lifetime region forms around the centre: it covers almost the entire wafer and resembles the defect structures observed in sample B of the boron-doped silicon (see Fig. 6d). The fact that the same defect structures are

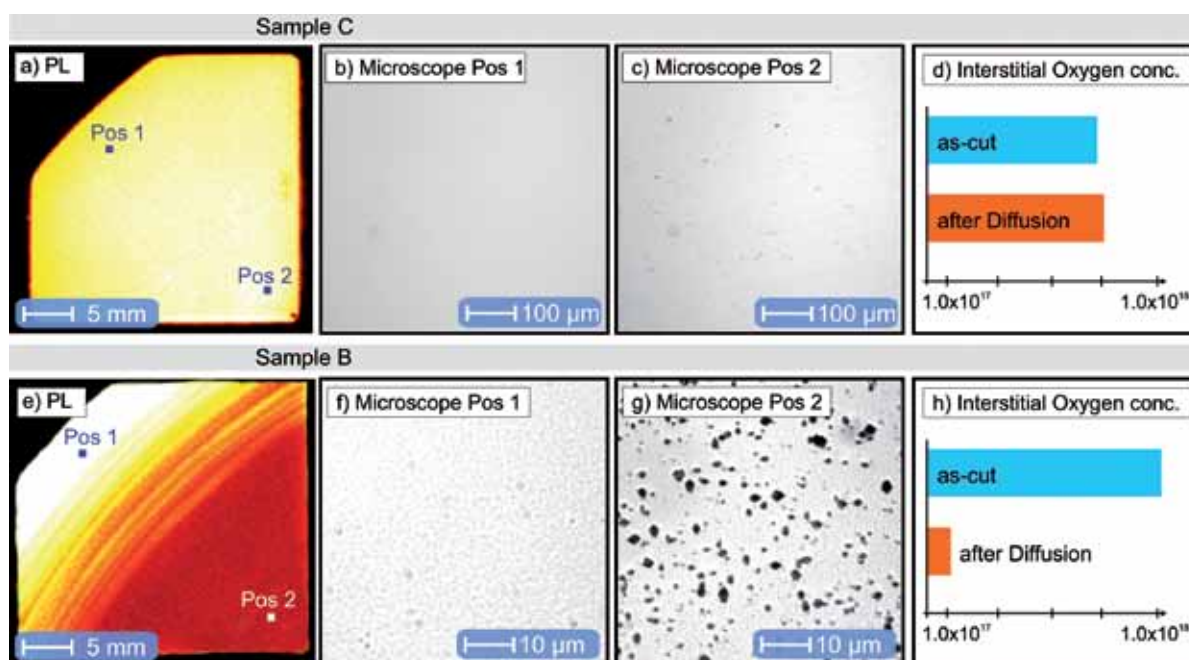


Figure 9. (a) PL image of sample C after preferential etching; (b,c) optical microscope pictures of the marked positions – no precipitates can be observed; (d) interstitial oxygen concentration of neighbouring samples of sample C; (e) PL image of sample B after preferential etching; (f,g) optical microscope pictures of the marked positions – the darker the PL image, the higher the density of precipitates; (h) interstitial oxygen concentration of neighbouring samples of sample B.

found in both gallium-doped and boron-doped silicon indicates that the formation of the observed severe ring defects is independent of the dopant, and is induced by more intrinsic effects such as oxygen precipitation after high-temperature treatments. Oxygen precipitates grow independently of the wafers' doping during high-temperature processing steps. That is why the observed phenomenon seems to be relevant for all Cz-Si materials.

“Oxygen precipitates grow independently of the wafers' doping during high-temperature processing steps.”

Defect characterization

To shed some light on the physical origin of the observed defect structures, a more detailed defect characterization was performed on adjacent wafers for selected material types. By using Fourier transform infrared (FTIR) spectroscopy, the interstitial oxygen content of neighbouring samples was measured in the as-cut state and after emitter diffusion. For wafers similar to sample C (without rings), the interstitial oxygen concentrations were measured to be $[O_i]=7 \times 10^{17} \text{cm}^{-3}$ in both states; for wafers similar to sample B (with rings), the concentrations changed from $[O_i]=1 \times 10^{18} \text{cm}^{-3}$ in the as-cut state to $[O_i]=1 \times 10^{17} \text{cm}^{-3}$ after emitter diffusion (see Figs. 9d and 9h). For the sample with ring

defects, the fact that the interstitial oxygen concentration is reduced during solar cell processing indicates that more oxygen precipitates are formed, which cannot be measured by means of an FTIR analysis.

In order to prove the presence of oxygen precipitates, the samples were polished and wet-chemically etched using the Sirtl etch [26]. Fig. 9(a) shows the PL image of sample C; the microscope pictures of small areas of the same sample can be seen in Figs. 9(b) and 9(c). Apart from dust

particles and a scratch, no precipitates are present. Fig. 9(e) shows the PL image of sample B with ring defects. For this sample, the images of the optical microscope (Figs. 9f and 9g) reveal that in the outer region of the wafer, with high PL signal, no precipitates are present, while in the inner region, with low PL signal, lots of precipitates can be found. Therefore, the drop in lifetime and efficiency of group B can be attributed to the presence of oxygen precipitates.

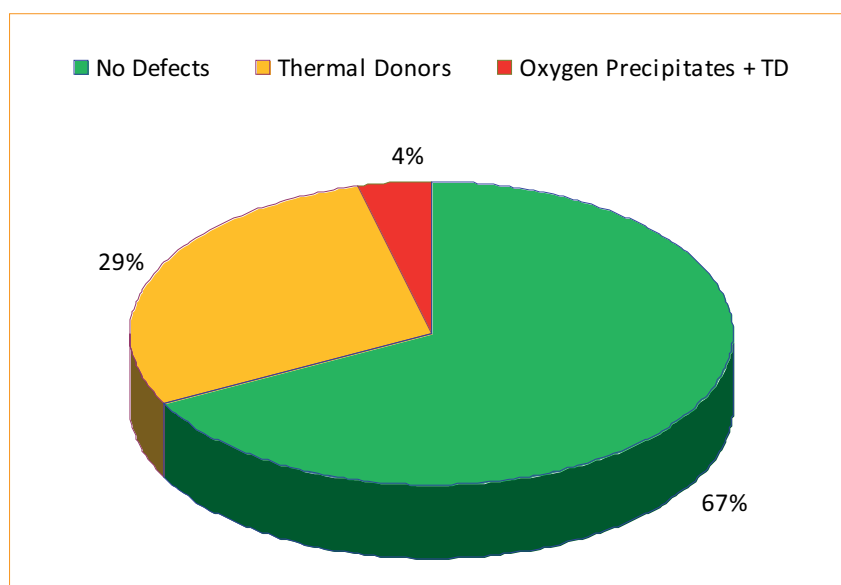


Figure 10. Statistics of the defects in commercially available Cz-Si wafers used at Fraunhofer ISE since 2010. The classification is based on PL imaging performed on random samples of all incoming wafers. Only two-thirds of the Cz-Si wafers are defect free; 29% exhibit thermal donors and 4% severe oxygen precipitates.

Statistical evaluation

In order to estimate, in a more quantitative way, the practical relevance of the defect classes discussed above, the IQC results obtained at Fraunhofer ISE were evaluated statistically. Since September 2010 all incoming Cz-Si wafers have had to pass the IQC based on PL imaging. Between 1 and 5% of the samples are selected randomly from each wafer box, and PL measurements are carried out. Our statistics are currently based on PL measurements of 1529 wafers, representing approximately 40,000 wafers.

Fig. 10 shows that ring structures were found in 33% of the investigated Cz-Si samples. Most of these ring structures could be identified as being related to harmless thermal donors, which vanish after high-temperature treatments. However, in 4% of the samples with ring structures in the as-cut state, the critical lifetime-limiting ring defects could be activated. These particular samples cannot be used for solar cell production, as the oxygen precipitates limit the solar cell efficiency to a low level. Although these statistics do not claim to be representative or precise, they strongly suggest that the observed phenomenon is highly relevant in terms of material yield.

Conclusion

This study has shown that commercially available Cz-Si materials labelled as 'high quality' may be affected by oxygen precipitates, which may reduce solar cell efficiency by 4% (absolute). Nucleation centres for oxygen precipitates have already been formed during crystallization; they strongly depend on the temperature cycles applied and may grow during high-temperature steps in the solar cell process, irrespective of the wafer doping. The critical defects appear throughout the production process as dark concentric rings in PL images.

Detection of oxygen precipitates in the as-cut state during incoming inspection is rather difficult, as the presence of harmless thermal donors can form similar patterns. Up till now, wafers that form efficiency-limiting oxygen precipitates during emitter diffusion could be detected with PL imaging in incoming inspections only if the presence of thermal donors could be excluded. If thermal donors cannot be excluded, reliable quality control after emitter diffusion is only possible using lifetime measurements or PL imaging.

Use of these results has allowed an incoming quality control based on PL imaging to be developed and introduced in the PV-TEC research line at Fraunhofer ISE. Two years of statistics have revealed that approximately 33% of all Cz-Si wafers show ring defects caused by thermal donors, and 4% form critical defects related

to oxygen precipitates, demonstrating the relevance of the phenomenon in terms of material yield.

Acknowledgements

We thank our colleagues at Fraunhofer ISE for their fruitful discussions and support in solar cell processing. This work was partially supported by the Fraunhofer Society under the framework of the ABICS-LUM project.

References

- [1] Fuyuki, T. et al. 2005, "Photographic surveying of minority carrier diffusion length in polycrystalline silicon solar cells by electroluminescence," *Appl. Phys. Lett.*, Vol. 86, p. 262108/1.
- [2] Trupke, T. et al. 2006, "Photoluminescence imaging of silicon wafers," *Appl. Phys. Lett.*, Vol. 89, p. 44107.
- [3] Chunduri, S.K. 2011, "Making the invisible visible: A market survey on luminescence imaging systems and cameras," *Photon Inter.* (January), p. 158.
- [4] Nagel, H. 2010, "Luminescence imaging – A key metrology for crystalline silicon PV," *Proc. 12th Worksh. Cryst. Si. Sol. Cell Mater. & Process.*, Breckenridge, Colorado, USA, p. 40.
- [5] Trupke, T., Nyhus, J. & Haunschild, J. 2011, "Luminescence imaging for inline characterisation in silicon photovoltaics," *physica status solidi (RRL)*, Vol. 5, p. 131.
- [6] Haunschild, J. et al. 2010, "Quality control of as-cut multicrystalline silicon wafers using photoluminescence imaging for solar cell production," *Solar Energy Mater. & Solar Cells*, Vol. 94, p. 2007.
- [7] Bothe, K. et al. 2010, "Determining the bulk lifetime of unpassivated multicrystalline silicon wafers," *Proc. 25th EU PVSEC*, Valencia, Spain, p. 204.
- [8] Sinton, R. et al. 2010, "The effects of sub-bandgap light on QSSPC measurement of lifetime and trap density: What is the cause of trapping?," *Proc. 25th EU PVSEC*, Valencia, Spain, p. 1073.
- [9] McMillan, W., Trupke, T. & Weber, J.W. 2010, "In-line monitoring of electrical wafer quality using photoluminescence imaging," *Proc. 25th EU PVSEC*, Valencia, Spain, p. 1346.
- [10] Demant, M. et al. 2010, "Analysis of luminescence images applying pattern recognition techniques," *Proc. 25th EU PVSEC*, Valencia, Spain, p. 1078.
- [11] Lawrenz, A. et al. 2010, "Photoluminescence lifetime imaging using LED arrays as excitation source," *Proc. 25th EU PVSEC*, Valencia, Spain, p. 2486.
- [12] Haunschild, J. et al. 2011, "Detecting efficiency-limiting defects in Czochralski-grown silicon wafers in solar cell production using photoluminescence imaging," *physica status solidi (RRL)*, Vol. 5, p. 199.
- [13] Cousins, P.J. et al. 2010, "Generation 3: Improved performance at lower cost," *Proc. 35th IEEE PVSC*, Honolulu, Hawaii, USA, p. 000275.
- [14] Rein, S. et al. 2001, "Electrical and thermal properties of the metastable defect in boron-doped Czochralski silicon (Cz-Si)," *Proc. 17th EU PVSEC*, Munich, Germany, p. 1555.
- [15] Schmidt, J. & Bothe, K. 2004, "Structure and transformation of the metastable boron- and oxygen-related defect center in crystalline silicon," *Physical Review B*, Vol. 69, p. 0241071.
- [16] Haunschild, J. et al. 2011, "Quality control of Czochralski grown silicon wafers in solar cell production using photoluminescence imaging," *Proc. 26th EU PVSEC*, Hamburg, Germany, p. 1025.
- [17] Marsden, K. et al. 1996, "Determination of the criteria for nucleation of ring-OSF from small as-grown precipitates in Cz-Si crystals," *Mater. Sci. & Eng. B*, Vol. 36, p. 16.
- [18] Porrini, M. et al. 2000, "Influence of Czochralski silicon crystal growth on wafer quality: An extensive investigation using traditional and new characterization techniques," *Mater. Sci. & Eng. B*, Vol. 37, p. 139.
- [19] Voronkov, V.V. & Falster, R. 1999, "Grown-in microdefects, residual vacancies and oxygen precipitation bands in Czochralski silicon," *J. Cryst. Growth*, Vol. 204, p. 462.
- [20] Meilwes, N. et al. 1994, "Thermal donors in silicon: An investigation of their structure with electron nuclear double resonance," *Semicond. Sci. Technol.*, Vol. 9, p. 1623.
- [21] Wagner, P. & Hage, J. 1989, "Thermal double donors in silicon," *Appl. Phys. A*, Vol. 49, p. 123.
- [22] De Kock, A.J.R., Roksnoer, P.J. & Boonen, P.G.T. 1975, "Formation and elimination of growth striations in dislocation-free silicon crystals," *J. Cryst. Growth*, Vol. 28, p. 125.
- [23] Föll, H. 1975, "Formation and nature of swirl defects in silicon," *Appl. Phys. A*, Vol. 8, p. 319.
- [24] Chen, L. et al. 2011, "Effect of oxygen precipitation on the performance of Czochralski silicon solar cells," *Solar Energy Mater. & Solar Cells*, Vol. 95, p. 3148.
- [25] Glatthaar, M. et al. 2010, "Spatially resolved determination of dark saturation current and series resistance of silicon solar cells," *physica status solidi (RRL)*, Vol. 4, p. 13.

[26] Sirtl, E. & Adler, A. 1961, "Chromsäure-Flußsäure als spezifisches System zur Ätzgrubenentwicklung auf Silizium", *Z. Metallkde.*, Vol. 52, p. 529.

About the Authors



Jonas Haunschild leads the luminescence imaging team at Fraunhofer ISE. He studied physics at the Philipp University of Marburg and received his diploma degree in 2007. He has been with ISE since 2008 and recently completed his Ph.D. on luminescence-based methods for quality control in industrial solar cell production.



Juliane Broisch is a Ph.D. student in the in-line measurement techniques and quality assurance group at Fraunhofer ISE. She studied physics at the

Albert Ludwig University of Freiburg and received her diploma degree in 2010.



Isolde E. Reis is a member of the luminescence imaging team at Fraunhofer ISE. She received her diploma degree in 1984 in crystallography from the Albert Ludwig University of Freiburg, and was awarded a Ph.D. in 1988 for her work on the recrystallization of polycrystalline Si layers.



Stefan Rein is the head of the in-line measurement techniques and quality assurance group at Fraunhofer ISE, which focuses on metrology, production control, solar cell simulation and new silicon materials. He received his diploma degree in physics in 1998 from the Albert Ludwig University of Freiburg, and

his Ph.D. degree in 2004 for work carried out at Fraunhofer ISE on lifetime spectroscopy for defect characterization of silicon for photovoltaic applications.

Enquiries

Fraunhofer Institute for Solar Energy Systems (ISE)
Department PV Production Technology and Quality Assurance (PTQ)
Emmy-Noether-Straße 2
79110 Freiburg
Germany

Tel: +49 (0) 761 4588 5563

Fax: +49 (0) 761 4588 9250

Email: Jonas.Haunschild@ise.fraunhofer.de